D15.8 Report on long term monitoring of DC GIS in presence of defects

DOCUMENT INFO SHEET

Document Name:	Report on long term monitoring of DC GIS in presence of defects
Responsible partner:	SuperGrid Institute
Work Package:	WP 15
Work Package leader:	Uwe Riechert
Task:	15.2
Task lead:	Armado Rodrigo Mor

DISTRIBUTION LIST

APPROVALS

	Name	Company
Validated by:		
Reviewer:		
Reviewer:		
Task leader:	Armando Rodrigo Mor	TU Delft
WP Leader:	Uwe Riechert	ABB Switzerland Ltd

DOCUMENT HISTORY

Version	Date	Main modification	Author
1.0			
2.0			

WP Number	WP Title	Person months	Start month	End month
15	HVDC GIS Technology Demonstrator	164.5	23	54

Deliverable Number	Deliverable Title	Type	Dissemination level	Due Date
15.8	Report on long term monitoring of DC GIS with defects	Report	Confidential[1]	M54

[1] only for members of the consortium (including the commission services)

LIST OF CONTRIBUTORS

Work Package and deliverable involve a large number of partners and contributors. The names of the partners, who contributed to the present deliverable, are presented in the following table.

PARTNER	NAME
ABB	Uwe Riechert, Michael Gatzsche
DNV GL	Cornelis Plet, Hong He
SGI	Caterina Toigo, Thanh Vu, Alain Girodet
TenneT	Maximilian Tuczek
TU Delft	Armando Rodrigo Mor, Luis Castro Heredia, Fabio Munoz

CONTENT

NOMENCLATURE

ABBREVIATION	EXPLANATION
D15.8	PROMOTioN deliverables 15.8
FN	FluoroNitrile
FK	FluoroKetone
HVAC	High Voltage Alternating Current
HVDC	High Voltage Direct Current
IEC	International Electrotechnical Committee
PD	Partial Discharge
PDIV	PD inception voltage
SF6	Sulfur Hexafluoride
UHF	Ultra High Frequency
WP	Work Package

This project has received funding from the European Union's Horizon 2020 research and innovation programme under grant agreement No 691714.

EXECUTIVE SUMMARY

The increasing penetration of renewable energy generation and the need of long distance power transmission brought more and more to focus on HVDC solution respect to the AC one. In addition due to the space saving and immunity to extreme weather conditions Gas Insulated Switchgear (GIS) are the preferred solution for the offshore platforms. The combination of the two technology, resulting in HVDC GIS, is thus fundamental in the context of future offshore meshed HVDC networks.

Nowadays, Sulfur hexafluoride (SF_6) is commonly used as insulation gas for high voltage equipment and it has been used in GIS since the 1960s. However it is classified in the Kyoto protocol list as one of the gas with high Global Warming Potential (GWP). In order to reduce the impact of SF_6 to the greenhouse effect, it is interesting to see if it is possible to replace SF_6 in high voltage equipment by an alternative gas with lower GWP. In the past few years researches have been conducted to find these alternatives. Among different solutions, the two fluorinated gases: $(CF_3)_2CFCN$ – Novec^{TM} 4710 (FN) and $CF_3C(O)CF(CF_3)_2$ – Novec^{TM} 5110 (FK) are selected as promising candidates as they present very high dielectric strength, non-flammability, and low GWP (2100 for pure Fluoronitrile and about 1 for pure Fluoroketone). Unfortunately they present high boiling point and they must be mixed with buffer gases, such as CO_2 or dry air, to be suitable for low temperature applications. These mixtures start to be applied as insulating medium in HVAC GIS and they present a great potential to be used in future SF_6 free HVDC GIS. Thus the monitoring and diagnostic method, in particular through PD measurement, should be investigated to ensure safe operation of future HVDC applications.

This document presents the experimental results about long term partial discharge behavior of defects with SF_6 and SF_6 alternative gases under DC voltage. Two kinds of defects: a protrusion and a metallic particle on insulator surface and different gases: SF_6, FN-CO_2 mixture, FK-Air mixture with different pressures were investigated with different measuring and monitoring systems such as conventional method, direct PD pulse current measurement, UHF and magnetic sensors. The PD behavior of different defects and a comparison of different gases were then reported.

This project has received funding from the European Union's Horizon 2020 research and innovation programme under grant agreement No 691714.

1 INTRODUCTION

1.1 MOTIVATION

Gas insulated switchgear (GIS) is a proven technology in high voltage alternating current (HVAC) system mostly driven by space saving and immunity to extreme weather conditions. With the increasing need of transmission over long distances high voltage direct current (HVDC) systems are more and more applied in respect to AC systems. In this context, HVDC GIS is an interesting solution to replace conventional substation especially in offshore platform, thanks to its compactness and its high reliability. Thus feasibility verification for the application of the GIS technology under DC voltage are increasingly conducted [1]-[3].

Since the 1960s, sulfur hexafluoride, SF_6, is the gas mostly used in GIS due to its excellent electrical properties such as high dielectric strength and very good interruption capability of electric arc. However, SF_6 is classified as one of the gases with very high greenhouse effect (global warming potential - GWP) and it has been included in the Kyoto Protocol list. In the recent years research on SF_6 potential substitutes has been performed in order to reduce its greenhouse effect. To be suitable for high voltage equipment the SF_6 alternative gases should have low GWP, no ozone depletion, high dielectric strength, arc quenching capability, heat dissipation and non-liquefaction at the functioning temperatures [4]. Dry air, N_2, and CO_2 are environmentally friendly gases and easy to handle. However, these gases have lower dielectric performance than that of SF_6, so the size of the equipment has to be increased. The mixing of SF_6 with these natural gases was a first approach to lower the environmental impact. However they cannot solve the greenhouse effect fundamentally due to the presence of SF_6.
Recently, new promising fluorinated gases from the fluoronitrile and fluoroketone families have been developed. In particular, the $(CF_3)_2CFCN$ – Novec^{TM} 4710 (FN) and $CF_3C(O)CF(CF_3)_2$ – Novec^{TM} 5110 (FK) are presenting high dielectric strength, non-flammability, low GWP and no ozone depletion. Unfortunately these compounds present high boiling point which is a drawback for their use as filling gas for low temperature electrical apparatus. Buffer gas must be used, as for example CO_2 and dry air, to reduce the liquefaction temperature of the final mixture [5].

Different gas mixtures with FN and FK into a buffer gas are today industrially investigated in AC GIS [6]-[8] and their application could be extended in the perspective of SF_6 free DC GIS development. Investigations are mainly focused on the dielectric strength and switching/interrupting performance of different SF_6 alternative gases [8]-[11] while little works have been addressed to the partial discharge (PD) behavior of such gases [12][13] which gives further information on the presence of defect and thus the dielectric strength. One can note that partial discharge measurement is considered as one of the most powerful monitoring and diagnostic tool for such equipment when the measurement is associated with algorithms for predicting defect recognition.

Up to now, there is some works related to the PD behavior under DC voltage but most of them were performed with small scale test setup and with standard gases such as N_2, air or SF_6 [14]-[15]. In most of the cases, the experiments are performed on small scale test setup that cannot be easily extrapolated to the full size GIS. To

This project has received funding from the European Union's Horizon 2020 research and innovation programme under grant agreement No 691714.

have a better understanding of the phenomena and sensitivity quantification, experiments need to be realized on the real size equipment.

Paper [15] presented the partial discharge inception voltage (PDIV) of a protrusion defect on high voltage conductor under DC voltage for N_2 and for SF_6 on real size test setup. According to the knowledge of the authors, there is only some works related to the PD behavior of SF_6 alternative gases/mixtures but all these studies were focused on AC PD. It is observed that the higher PD amplitude is observed during negative period of voltage for SF_6 gas while the opposite tendency was observed for FN-CO_2 mixture [12]. It is thus essential to investigate and to understand the contribution of gas composition/mixture to the PD behavior under DC voltage as the mechanism and the behavior of PD impulse might change depending on the applied voltage and polarity. Moreover, for an effective monitoring system and a reliable design of SF_6 free HV apparatus, it is mandatory to compare the PD in SF_6 and alternative gases with same dielectric strength as the design of SF_6 free apparatus should require optimized dimension. For this purpose, in PROMOTioN WP15 framework, the deliverable D15.7 [16] presents a study on partial discharge behavior of SF_6 and its alternative gases such as fluoronitrile (Novec^{TM} 4710) – CO_2 (FN-CO_2) mixtures and fluoroketone (Novec^{TM} 5110) – dry air mixture (FK-Air) with protrusion defect on high voltage conductor and metallic particle on insulator surface inside a real size GIS, and under DC voltage. The PD inception voltage (PDIV) and the PD characteristics are then compared between SF_6 and alternative gases at the same SF_6 equivalent dielectric strength. The effects of gas composition, gas mixing ratio, gas pressure, applied polarity on the PDIV and the PD behavior are analyzed. In addition to the conventional method, supplementary information with UHF, light emission, high frequency current transformers (HFCT) methods are also provided.

According to the author's knowledge, there is no study about long term behavior of partial discharge under DC voltage while under DC voltage, physical phenomena can change with time due to the transition of the electric field from a capacitive distribution to resistive distribution, which can vary from days to months [17]. Moreover, the phenomena of charge accumulation (on both surface and volume) can strongly impact the electric field distribution. Therefore, the aim of this deliverable is to give an overview about PD long term behavior of not only SF_6 gas but also for SF_6 alternative gases with two kind of defects: protrusion on HV conductor and metallic particle on spacer's surface.

1.2 RELATION TO PROMOTION

PROMOTioN is a European Union project which seeks to develop meshed HVDC offshore grids on the basis of cost-effective and reliable technological innovation in combination with a political, financial and legal regulatory framework. PROMOTioN is divided into different work packages. Subsequently, each work package consists of different tasks.
This document serves as the eighth deliverable D15.8 of work package WP15 "DC GIS technology demonstrator". It is a part of task 15.2: Develop monitoring and diagnostic method and applicability of SF_6 alternatives.

This project has received funding from the European Union's Horizon 2020 research and innovation programme under grant agreement No 691714.

1.3 DOCUMENT STRUCTURE

The document is structured as follows: In chapter 2 test setup and PD measurement procedure are presented while in chapter 3 the PD behavior of different defects and the comparison in term of PD behavior for SF_6 and SF_6 alternative gases are illustrated. The document finishes with a conclusion in Chapter 4, where the results obtained above are summarized.

This project has received funding from the European Union's Horizon 2020 research and innovation programme under grant agreement No 691714.

2 TEST SETUP & MEASUREMENT PROCEDURE

2.1 INSULATING GASES

The choice of insulating gases are explained in [16] and are summarized in Table 1. Three gases with equivalent dielectric strength are thus investigated: SF6 at 5 bar abs, 6.6% Novec^{TM} 5110/Dry Air mixture at 7.5 bar abs and 10% Novec^{TM} 4710/CO_2 mixture. One can note that the SF_6 equivalent dielectric strength is calculated on the basis of critical reduced electric field under homogeneous electric field configuration. The gas mixtures are prepared according to the recommendation of gas provider in order to ensure the uniformity of the mixture.

Gas	Pressure (bar abs)
SF_6	**5 (reference)**
Novec^{TM} 5110/Dry Air Mixture (6.6 % Novec^{TM} 5110)	**7.5**
Novec^{TM} 5110 (pure)	0,5
Dry Air (pure)	7
Novec^{TM} 4710/CO_2 Mixture (10 % Novec^{TM} 4710)	**6.5**
Novec^{TM} 4710 (pure)	0.65
CO_2 (pure)	5.85

Table 1: Investigated gas mixture with the pressure which leads to the same dielectric strength like SF_6 at 5 bar.

2.2 TEST SETUP, DEFECTS AND TEST LABORATORY

The breakdown of insulating materials, one of the most usual reason of failure for GIS in service [18], is most often caused by the presence of defects inside GIS. They can be generated during fabrication process, assembling phase or during close/open operation of disconnector or earthing switch or circuit-breaker. As known PD measurements is an effective tool for defect monitoring and identification. Thus the understanding of the defect behavior under long term voltage application is therefore essential to prevent failure of GIS

The interest of the conducted investigations is the comparison of the PD long term behavior between SF_6 and alternative gases to SF_6 in DC voltage. Two different types of defect, among the most common defects in GIS, were thus introduced inside the test compartment to generate PD activity. Those defects are:

- Protrusion on high voltage conductor: a tungsten needle with 10 mm of length, 0.5 mm of diameter and 50 µm of tip radius on the HV conductor.
- Metallic particle on solid insulator surface: a tungsten needle of 20 mm of length and 0.5 mm of diameter was glued close to the triple point, on the cylindrical insulator surface. It exceeds 10 mm the high voltage electrode.

PROMOTioN – Progress on Meshed HVDC Offshore Transmission Networks

This project has received funding from the European Union's Horizon 2020 research and innovation programme under grant agreement No 691714.

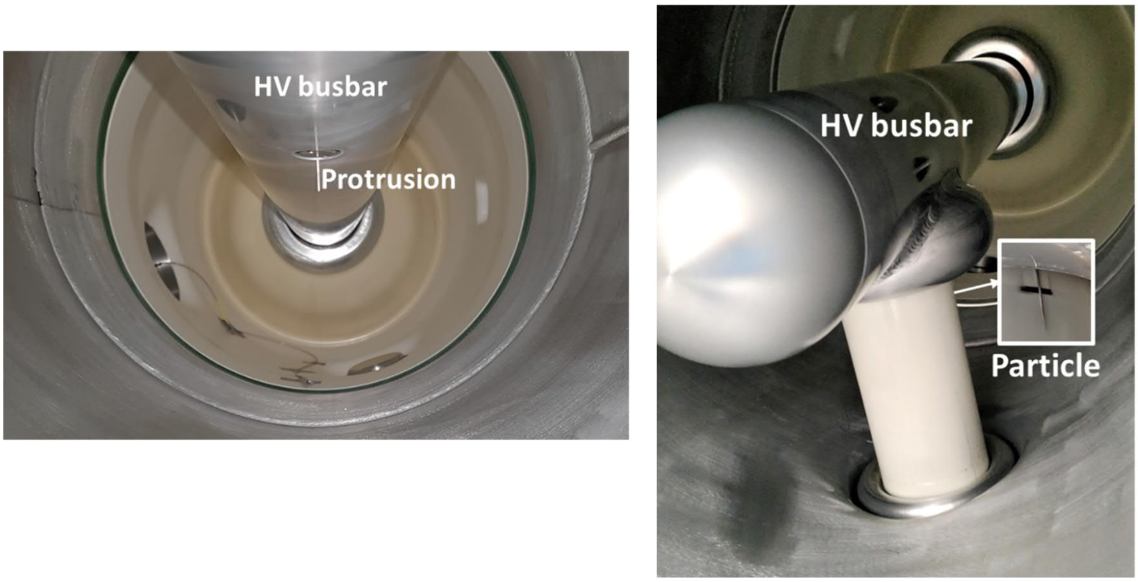

Figure 1: Installation of the defect in the test compartment

Should be noted that the length of these defects is relatively large respect to usual defect size inside apparatus. However such length permits to facilitate the comparison of PD behavior of SF_6 alternative gases due to the higher PD amplitudes at the lower PD inception voltages.

To perform long term test, a test rig was built to apply during long term the DC voltage on the test setup. The whole system is insulated in SF_6 gas to reduce ambient noise interference. The AC voltage generated by AC transformer is converted to DC voltage thanks to a diode rectifier. The noise of the DC source is about 500 fC. The installation of test setup in the test rig is illustrated in Figure 2.

This project has received funding from the European Union's Horizon 2020 research and innovation programme under grant agreement No 691714.

Figure 2: Test setup with two independent test compartments

2.3 MEASURING SYSTEMS

Due to the lack of knowledge on DC partial discharge behavior, especially for SF_6-free alternative gases, different PD measuring systems are used, as showed in Figure 3. When a PD occurs in gas different signals can be generated such as electric current and electromagnetic wave emission. The following systems are thus used to capture different kind of PD signals: Conventional system, PD pulse signal and magnetic sensor for electric current, and Ultra High Frequency (UHF) antenna for electromagnetic wave.

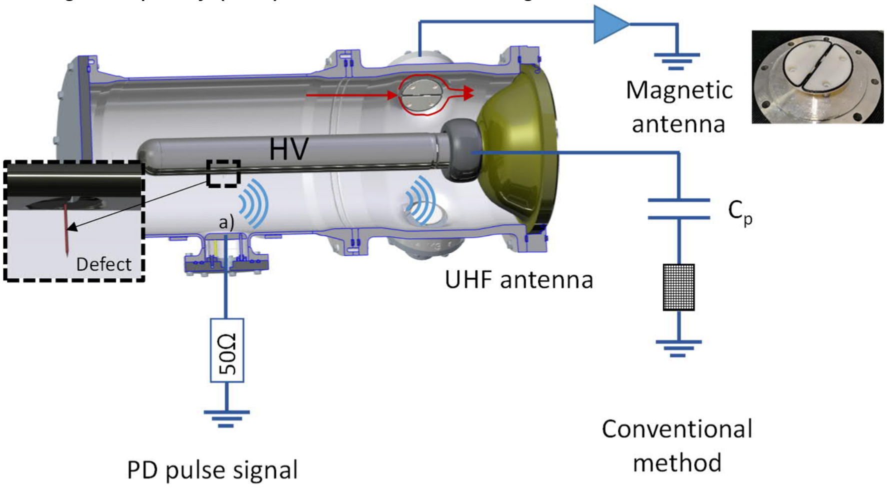

Figure 3: Test setup with different measuring systems: mesuring electrodes (a) for the PD pulse signal, conventioal system, UHF antenna and magnetic antenna.

PROMOTioN – Progress on Meshed HVDC Offshore Transmission Networks

This project has received funding from the European Union's Horizon 2020 research and innovation programme under grant agreement No 691714.

The detail about different measuring techniques can be found below.

2.3.1 CONVENTIONAL METHOD

Test setup compliant with IEC 60270 is used, as reported in Figure 4. A coupling capacitor of 500 pF is connected to the test compartment and thanks to the measuring impedance Omicron CLP542, the PD conventional measurement compliant with the IEC 60270 [19] is performed.

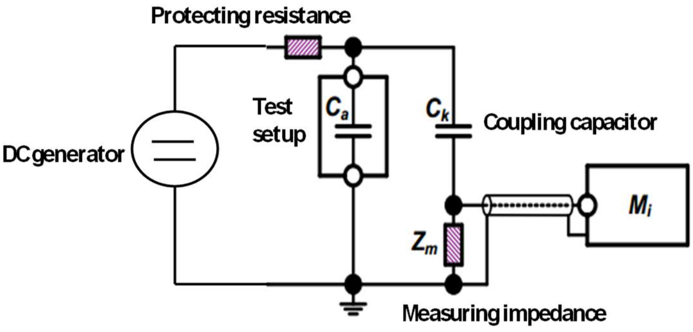

Figure 4: Circuit for DC PD measurement

2.3.2 PD PULSE SIGNAL

When PD occurs, current pulses are generated. A measuring electrode, denoted (a) in Figure 3, is thus installed in front of the defect and insulated from ground to measure explicitly the PD pulses. As the PD current is the sum of a DC and a pulse component, a capacitor of 100 nF is inserted in series between the measuring electrode and a Femto HCA-40M-100K-C amplifier to collect only the high frequency signal components.

2.3.3 UHF SYSTEM

PD activities will also generate electromagnetic waves, which will travel inside GIS. As the external electromagnetic wave disturbances are mainly in low frequency range (except the frequency range for e.g. the mobile phone), the PD signal noise ratio is very good at ultra-high frequency range. In order to overcome the effect of disturbance, present at low frequencies in GIS, the ultra-high frequency (UHF) measuring method, ranging from 300 MHz to 3 GHz, has been extensively used due to its high signal/noise ratio and high resilience to the electromagnetic interference (EMI).

The UHF method is based on capacitive couplers (electric antennas), tuned at the ultra-high frequency range and installed in the multiple windows present in the GIS enclosure. The GIS enclosure itself acts as a Faraday cage, shielding the capacitive couplers from external electromagnetic interferences. The high sensitivity and the low background noise provide by the UHF method has led to promote its application as a standard for on-line monitoring on AC GIS/GIL.

An UHF antenna is thus installed inside test setup. The signal coming from this antenna is connected to a high pass filter and then to a 28 dB amplifier with the bandwidth of 300 MHz – 2000 MHz. The obtained waveform is recorded thanks to an oscilloscope Tektronix DP07000.

This project has received funding from the European Union's Horizon 2020 research and innovation programme under grant agreement No 691714.

2.3.4 MAGNETIC ANTENNA

Recent research on alternatives for HVDC GIS conducted by TU Delft [20] is focusing on magnetic detection of PD signals. Magnetic field sensors, tuned at the high frequency range (10 MHz – 100 MHz), are placed in the existing windows of the GIS enclosure in replacement of the UHF couplers. At this frequency range the PD currents can travel along the GIS with enough amplitude and the currents can be picked-up by the coils of this sensor. The one-turn pick-up coil comprises two hemi-loops arrangement that outputs two signals of similar magnitude but opposite polarity. The different polarity of the signals is used to discriminate between disturbances and actual PD signals [20]. Magnetic field sensor is thus an interesting solution to measure and monitor PD in GIS due to its possibility to compute apparent charge, to increase signal/noise ratio by signal processing (double coil principle) and to reduce the measuring hardware requirements as it works at much lower frequency than UHF method [21].

A magnetic field sensor with double pick-up coils, provided by TU Delft in the framework of PROMOTioN WP 15 is as well inserted in the test setup. The current signals are amplified by a Femto HCA-40M-100K-C amplifier. A parallel 100 nF decoupling capacitor is connected in series between the antenna and the amplifier to block the DC component of current and to reduce noise. The signals are then recorded by an oscilloscope Tektronix DP07000.

The installation of protrusion defect and metallic particle on insulator's surface is illustrated in Figure 1.

2.4 MEASUREMENT PROCEDURE

Before the test, the different measuring systems were calibrated or their sensitivity is verified. The conventional system was calibrated according to IEC 60270 thanks to the Omicron CAL 542 calibrator. As there is no meaning to compute the PD amplitude for UHF system, the UPG 620 pulse generator is used to check the sensitivity of UHF antenna according to [22]. The background noise level of the signals given by PD pulse current, magnetic sensor and UHF sensor were also recorded.

An example of the background noise measured by the conventional method is reported in Figure 5. One can identify two noise behaviors:

- Installation noise: about 500 fC.
- Noises caused by the HV source diodes commutation: higher level but they are easy to identify.

PROMOTioN – Progress on Meshed HVDC Offshore Transmission Networks

This project has received funding from the European Union's Horizon 2020 research and innovation programme under grant agreement No 691714.

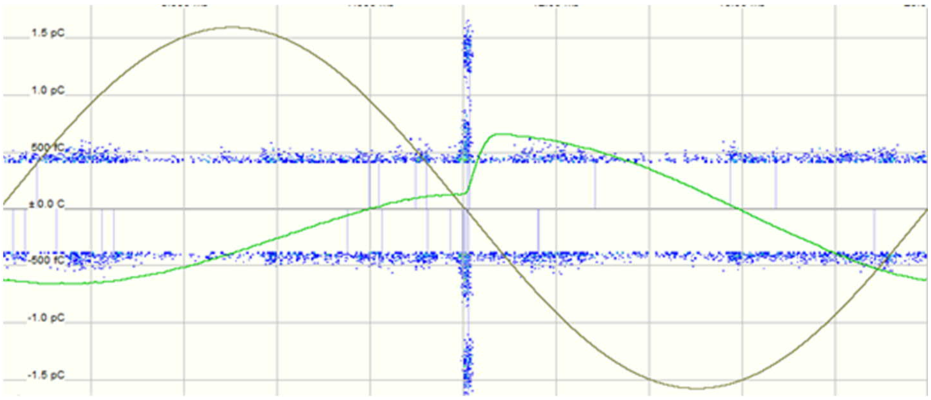

Figure 5: Background noise measured at +240 kV measured by the conventional measurement system

The long term PD measurement of different defects in DC voltage was then carried out as following:

- Protrusion defect: application of +/-150 kV during at least one week for each polarity.
- Metallic defect on insulator surface: application of +/-230 kV during at least one week for each polarity.

For each test configuration (gas nature and gas pressure) PD measurements were carried out during at least 15 minutes, one time per day.

This project has received funding from the European Union's Horizon 2020 research and innovation programme under grant agreement No 691714.

3 RESULTS

3.1 PROTRUSION HV BUSBAR

3.1.1 OBSERVATION

To investigate and compare the PD behavior of protrusion under DC voltage between SF_6 and SF_6 alternative gases, PD measurements were carried out at different voltage polarity, with different gas compositions and gas pressures using all measuring systems presented in 2.3. An example of PD measurement with the conventional system is reported in Figure 6 for the 10% FN mixture at +150 kV. One can note that, as already observed in [16] the PD generated by the protrusion defect is continuous and the apparent charge are almost constant during all the application time.

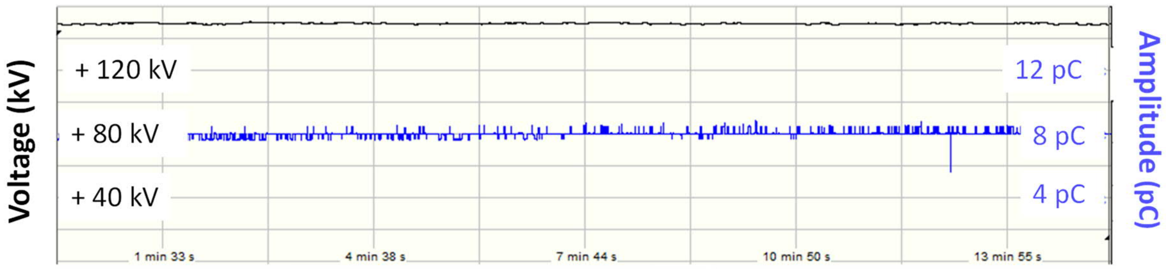

Figure 6: Example of signal recorded by the conventional measurement for the protrusion defect in FN-CO_2 10% mixture at + 150 kV.

An example of signal generated by the protrusion defect recorded by the other applied measuring systems (current measurement, UHF and magnetic sensor) is reported in Figure 7. One can note that the partial discharge can be detected simultaneously by the conventional method as well as by direct current measurement, magnetic antenna and UHF antenna. However, this is not always the case, especially when the PD amplitude is low (<2 pC). Indeed it has been observed in [23] that, depending on the gas nature and the frequency content of the generated PD signal, the partial discharges are less easily detected by the UHF and magnetic antenna either if PD signal in the current pulse measurement is detected. With low discharge amplitude, the electromagnetic wave and the current pulse on the enclosure will be also very small, it is thus more difficult for the PD to be picked-up by magnetic antenna and UHF antenna.

This project has received funding from the European Union's Horizon 2020 research and innovation programme under grant agreement No 691714.

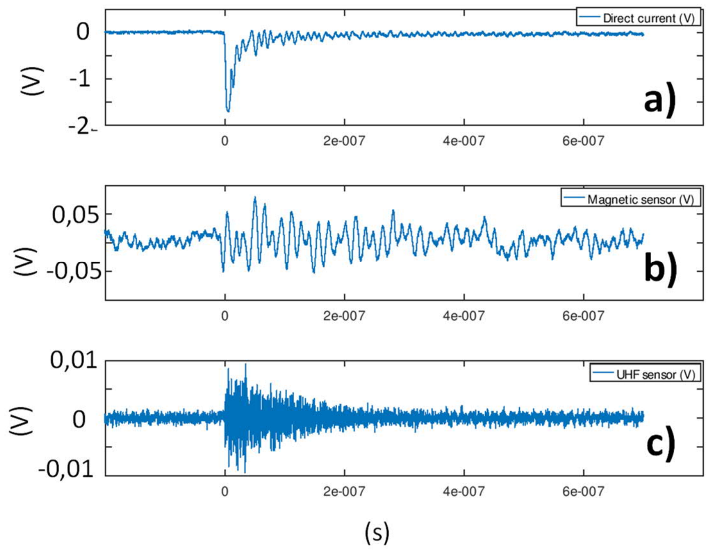

Figure 7: Example of signal recorded by direct current measurment (a), one coil of the magnetic sensor (b) and UHF sensor (c) for protrusion defect in SF_6 under negative polarity. The apparent charge is ~7 pC.

To facilitate the comparison between gases, only results issued from conventional method will be reported hereafter. More information about other methods will be presented in the comparison of measuring systems section 3.3.2. Figure 8 shows, as an example, the evolution of PD amplitude and PD repetition frequency for SF_6 in both positive and negative polarity.

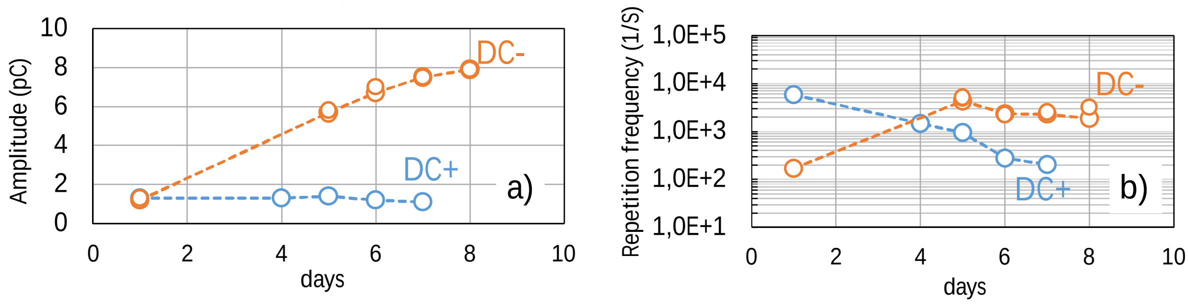

Figure 8: Evolution of PD amplitude and PD repetition frequency in function of time for SF_6. (a) PD amplitude and (b) PD repetition frequency

As illustrated in Figure 8, the PD amplitude given by conventional method is higher in negative polarity. This statement is in accordance with the results, for SF_6, presented in [16]. One can also underline that the PD amplitude increases with the voltage application time in negative polarity while it remains constant in positive polarity. Concerning the PD repetition frequency, it increases before reaching a stabilized value in negative polarity while it decreases in positive polarity.

Concerning the studied SF_6 alternative gases, the evolution of PD amplitude and PD repetition frequency are reported in Figure 9 for FN-CO_2 10% mixture and FK-Air 6.6% mixture. Like SF_6, the PD amplitude changes with time and the tendency depends strongly of the applied voltage and the gas composition.

This project has received funding from the European Union's Horizon 2020 research and innovation programme under grant agreement No 691714.

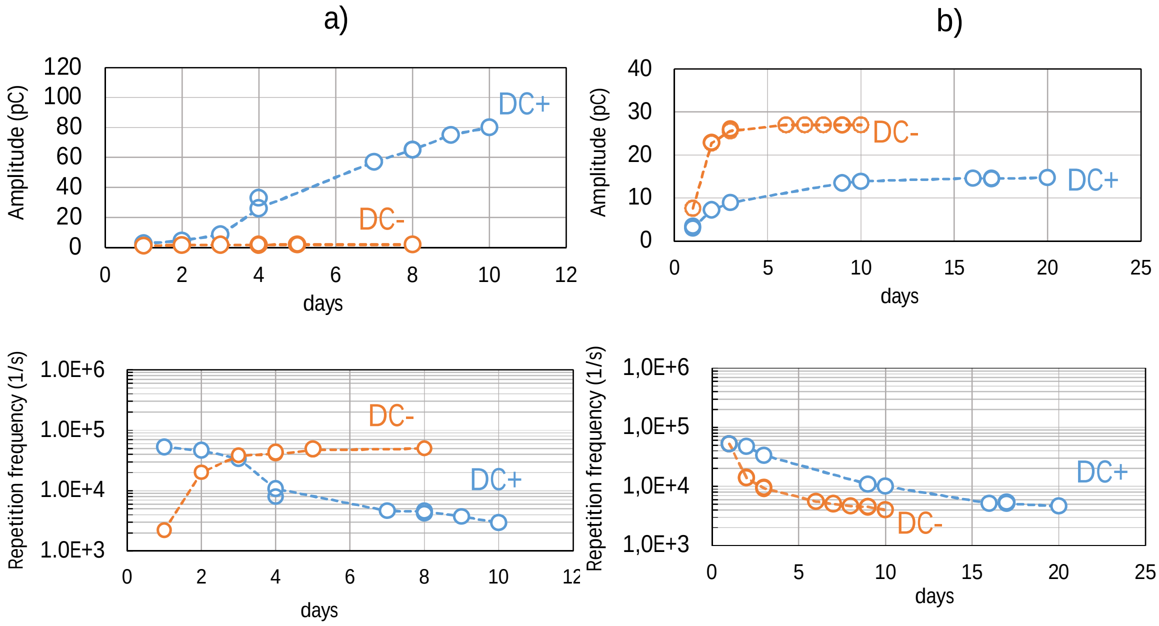

Figure 9: Evolution of PD amplitude and PD repetition frequency in function of voltage application time. (a) FN-CO_2 10% and (b) FK-Air 6.6%

3.1.2 GAS COMPARISON

The comparison between gases is presented in Figure 10.The PD amplitude (a, b) and the repetition frequency (c, d) change with time but depending on the gas nature and the DC polarity the behavior is not the same for the different gases/mixtures. One can observe that under positive polarity SF_6 presents the lowest PD amplitude among the others. The highest PD amplitude, after the continuous voltage application is observed under positive polarity for the FN-CO2 10% mixture. Under negative polarity is the FK-air 6.6% mixture that presents the highest PD amplitude.

Regarding the PD repetition frequency, as already observed in [16], the tested alternative gases present higher PD repetition frequency respect to SF_6. The repetition frequency always decrease for all gases under positive polarity while it increases under negative polarity for SF_6 and the FN-CO_2 10% mixture while it decreases for the FK-air 6,6% mixture.

A discussion about the possible causes for these behaviors with time is reported in the following chapter.

This project has received funding from the European Union's Horizon 2020 research and innovation programme under grant agreement No 691714.

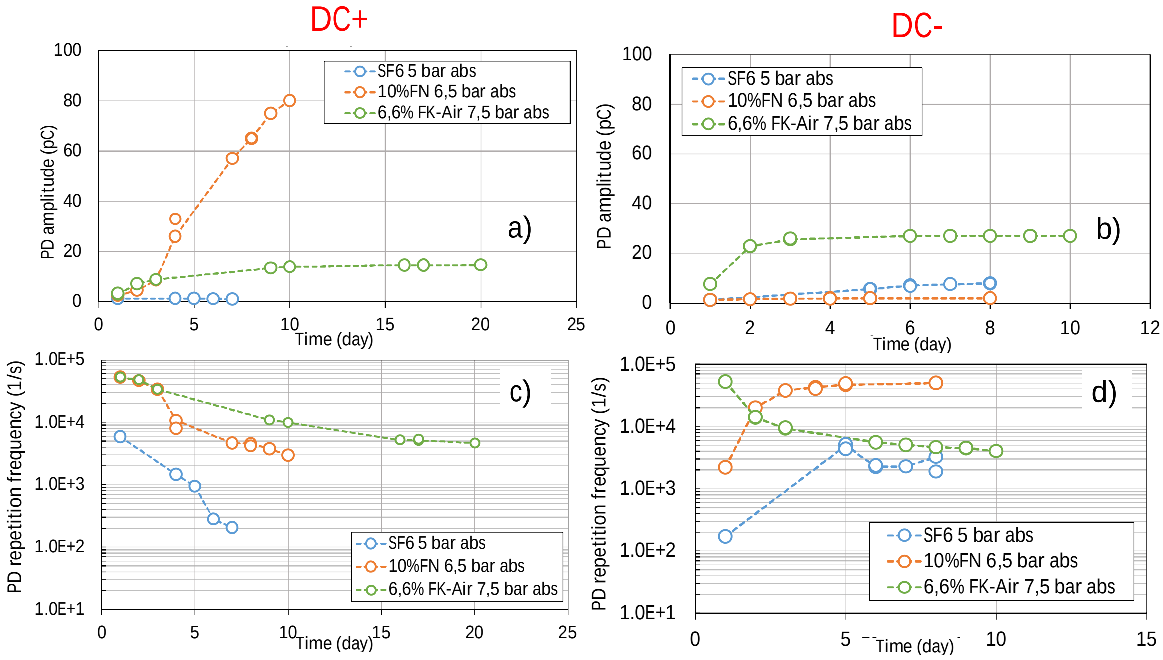

Figure 10: PD behavior comparison between SF_6, $FN\text{-}CO_2$ 10% mixture and FK-Air 6.6% mixture. (a), (c) positive polarity and (b),(d) negative polarity. (a), (b): PD apparent charge and (c), (d): PD repetition frequency. Protrusion defect of 1 cm and applied voltage: 150 kV.

3.1.3 SUMMARY & REMARK

As observe in chapter 3.1.2 the PD behavior changes with time, including PD amplitude and PD repetition rate. The PD amplitude increases with time before reaching a stabilized value after some days. Concerning the PD repetition rate, it changes also with time but the tendency depends a lot on the gas composition and the applied voltage. For example, in negative polarity the PD repetition rate increases with voltage application time in SF_6 and $FN\text{-}CO_2$ 10% while it decreases with voltage application time in FK-Air 6.6%. In positive polarity, the three investigated gases give the same tendency: PD repetition rate decreases with time.

This project has received funding from the European Union's Horizon 2020 research and innovation programme under grant agreement No 691714.

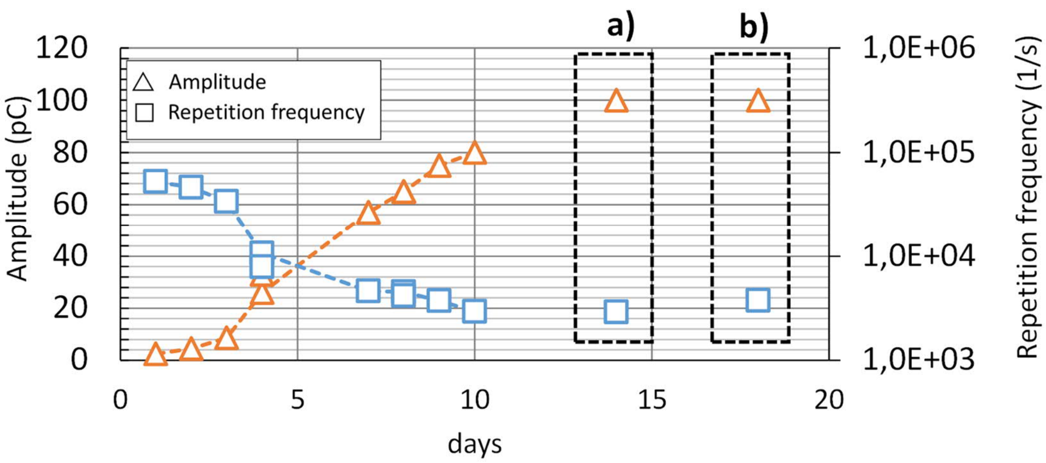

Figure 11: PD amplitude and repetition frequency variation for the 10% FN-CO_2 mixture: a) the voltage is reapplied after four days without voltage applications, b) the gas is recovered and refilled before applying again the voltage.

The evolution of PD amplitude in function of time is quite hard to explain. One of the possible reason is the change of gas composition in function of time with partial discharge activity. To have more detail about this possibility, at the end of the tests, the voltage has been interrupted voluntarily during different times, from some minutes to some days to observe the PD behavior. If the change of PD behavior is caused by the gas composition change without voltage and thus PD activities, the gas composition will come back to the initial state and thus the initial PD behavior should be observed. However, the PD amplitude remains always the same before and after voltage interruption, regardless the time. Moreover, the same tendency was also observed after recovering and refilling with new gas before reapplying the voltage. An example is shown in Figure 11 where the PD amplitude and the repetition frequency are measured, for the 10% FN-CO_2 mixture, reapplying the voltage after a stop of four days (measure a) and after the recovering and refilling with new gas (measure b). This suggests that the evolution of PD amplitude is not due to the change of gas properties/compositions under DC voltage but more likely by modification of the defect. Indeed, to confirm this, photos of the tungsten protrusion are taken after long term test for each gas and voltage polarity and compared with the photo of the point before the test. The photos of different needles before and after long term PD test are presented in Figure 12, Figure 13 and Figure 14 respectively.

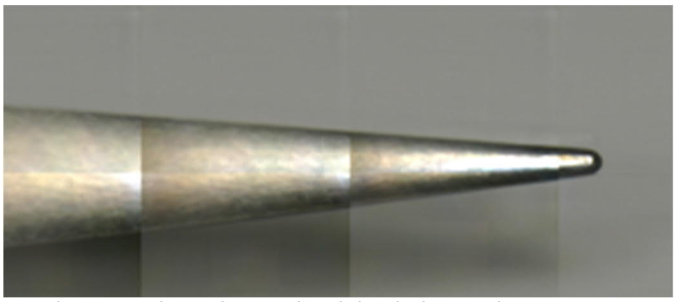

Figure 12: Photo of protrusion defect before PD long term test.

This project has received funding from the European Union's Horizon 2020 research and innovation programme under grant agreement No 691714.

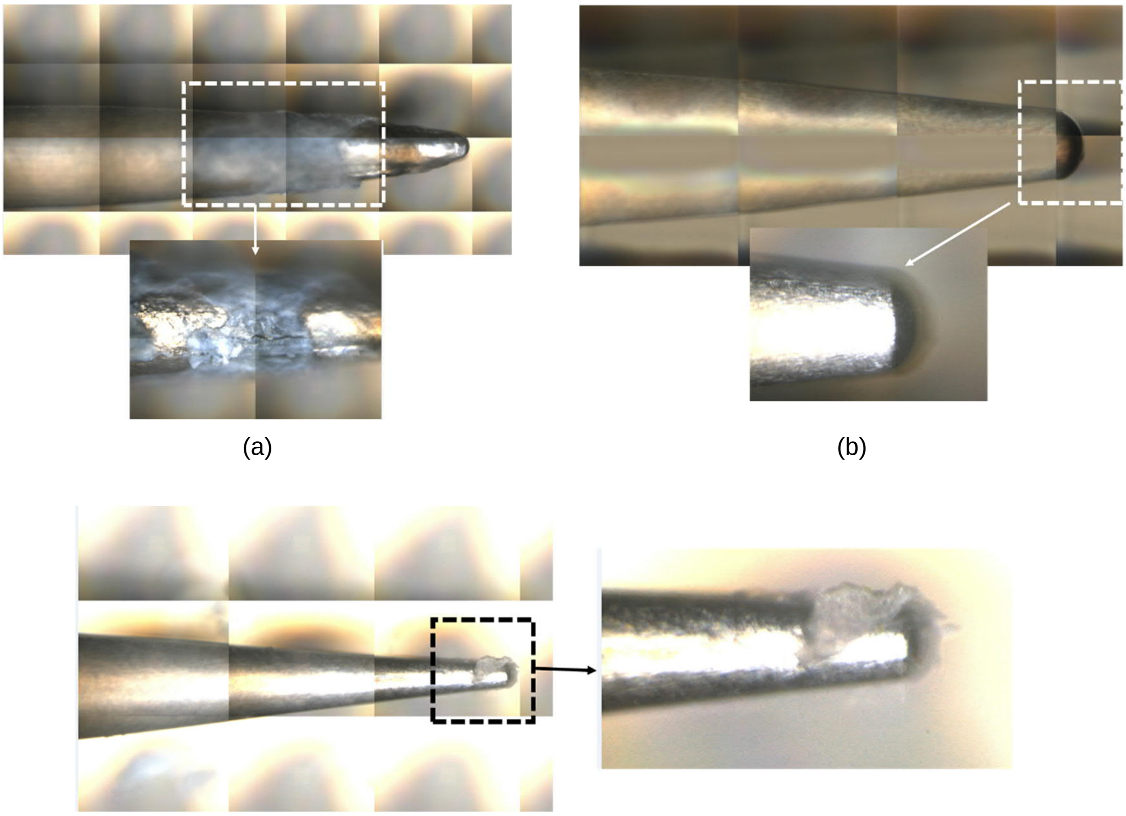

(c)

Figure 13: Protrusion defect after PD long term test in negative polarity for different gases. (a) SF_6, (b) FK-Air 6.6% and (c) FN-CO2 10%. Applied voltage: -150 kV.

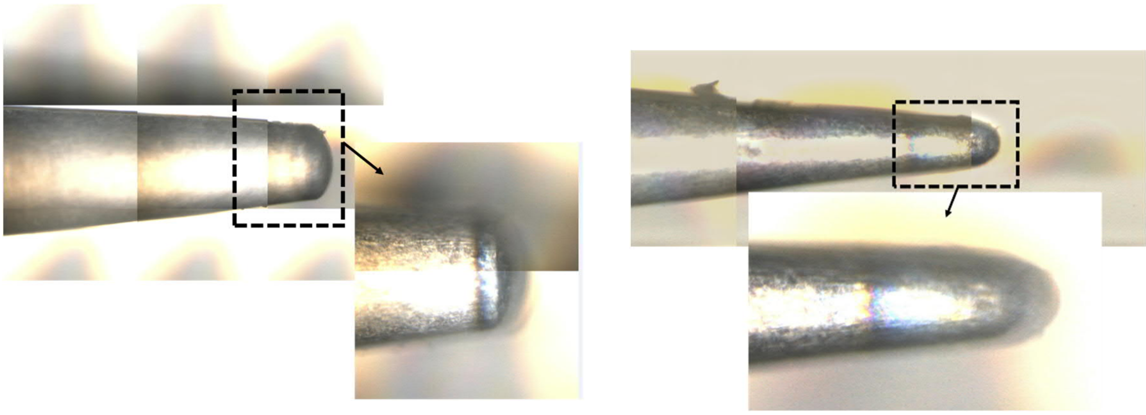

(a) (b)

Figure 14: Protrusion defect after PD long term test in positive polarity for different gases. (a) FK-Air 6.6% and (b) FN-CO_2 10%. Applied voltage: +150 kV.

Comparing the needle after the test in negative polarity, in Figure 13, one can note some differences in function of gas. Indeed the needle after the test in SF_6 presents a material pull out, see zoom in Figure 13a. A material pull out is also observed in FN-CO_2 10% mixture but in another position, see Figure 13c. For the needle after the test in FK-air 6.6 % mixture there is no evidence of material melting but the point is eroded, see zoom in Figure 13b. Also after the tests in positive polarity there is no evidence of material pull out but the points are eroded and

This project has received funding from the European Union's Horizon 2020 research and innovation programme under grant agreement No 691714.

a ring scorch mark are visible at the needle termination, see zoom in Figure 14a and b respectively for FK-air 6.6% and FN-CO_2 10% mixtures. Investigation with IRTF spectroscopy have been conducted to investigate the nature of the observed material pull out to confirm if it comes from a surface melting process but unfortunately, due to the 3D geometry were not concluding.

3.2 METALLIC PARTICLE ON INSULATOR SURFACE

3.2.1 OBSERVATION

Unlike protrusion defect where continuous PD signals are almost constant during the whole measurement time, the metallic particle on insulator surface generates PD signal during a relatively short time before extinction. An example of PD apparent charge evolution in function of time is shown in Figure 15 for FN-CO_2 10% in positive polarity.

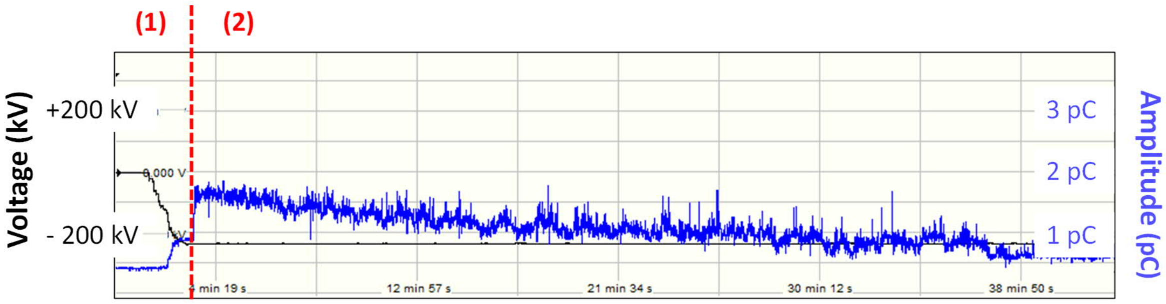

Figure 15: Evolution of PD apparent charge in function of time in FN-CO_2 10%. Applied voltage -230 kV.

One can distinguish two phases in Figure 15: (1) voltage raise and (2) constant voltage. During the first phase, the PD apparent charge increases with the voltage. When the voltage exceeds the PDIV, the PD apparent charge reaches a level of about 2 pC. When the applied voltage is constant, the PD apparent charge is not stable. Indeed, it decreases with the increase of time (phase 2 - Figure 15). At the first moment, the PD apparent charge is about 2 pC and it remains at only 700 fC after 35 minutes under -230 kV DC. This behavior is already observed in [16] for the metallic particle on insulator surface. When PD activities are presents, the metallic particle generates charges and these charges are then deposited on the insulator surface. The surface charges, in their turn, decreases the electric field on metallic particle ends and then decrease/stop the PD activities. The time needed to reach the final state where no more PD activity is observable depends on the gas and solid insulator characteristics. The deposited charges, with the time, can be evacuated via gas conduction, surface and volume conduction of solid dielectric, leading to higher electric field on metallic particle end and PD activity could start again. An example is reported in Figure 16 for SF_6 under negative polarity. The recorded PD amplitude is about 1.2 pC just after voltage application but it decreases to a value very close to ambient noise level, about 0.75 pC 9 minutes after (**Error! Reference source not found.**a). The PD amplitude is about 1 pC and 0.9 pC one day after and three days after as illustrated in Figure 16b and Figure 16c respectively.

PROMOTioN – Progress on Meshed HVDC Offshore Transmission Networks

This project has received funding from the European Union's Horizon 2020 research and innovation programme under grant agreement No 691714.

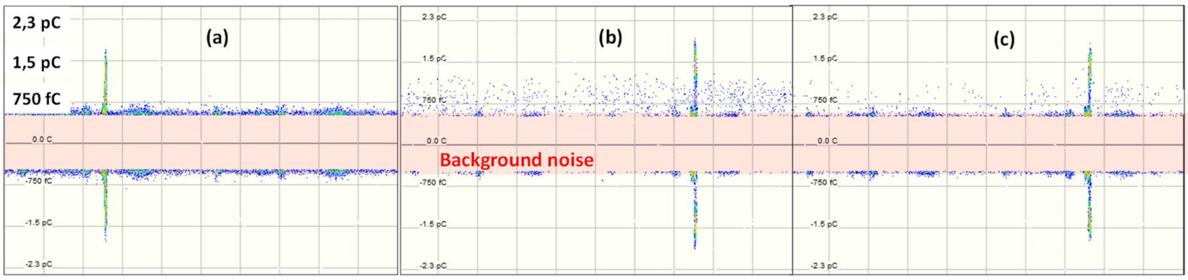

Figure 16: Evolution of PD activivty in SF_6 (applied voltage -230 kV): a) after 9 minutes of the first voltage application , b) After 1 day and c) after three days. The shown discharges are relative to 2 minutes.

Concerning the PD repetition frequency, just after the voltage application, a lot of PD activities can be recorded. However, as explained above with long time application, PD activities decrease and in this case very small number of PD pulses can be recorded. As example, after 24 h of voltage application only 131 pulses are measured in 40 minutes for the 10% FN- CO_2 mixture under negative polarity, see Figure 17.

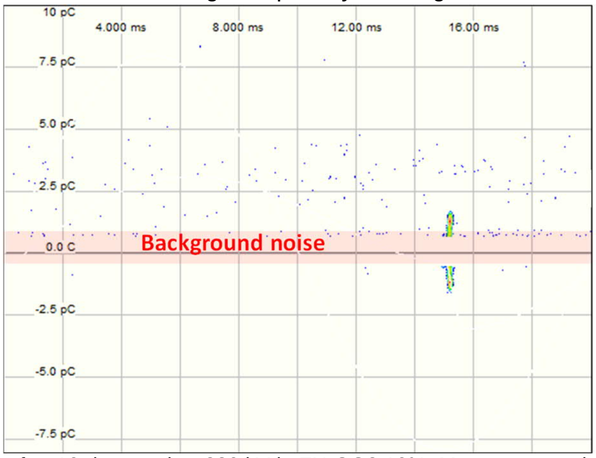

Figure 17: PD apparent charge after 10 days under -230 kV in FN-CO2 10%. Measurement duration: 40 minutes. Number of pulses except the PD due to diodes commutation: 131.

One can also underline that it is very hard to capture the unstable behavior of PD in function of time, especially for conventional method, due to the fact that the measurements take place only during some of ten minutes per day. To have a full image of PD behavior of metallic particle on insulator surface, an effective real time monitoring system which is able to record permanently low amplitude PD, is mandatory.

As presented above after a certain time of application of the voltage the partial discharge amplitude decrease significantly to values that are close to the background noise of the installation. To study about charge deposition and charge relaxation on insulator surface, we tried to stop the voltage during at least 15 minutes and then reapply it again. The PD apparent charge before and after voltage interruption are presented, as example, in Figure 18.

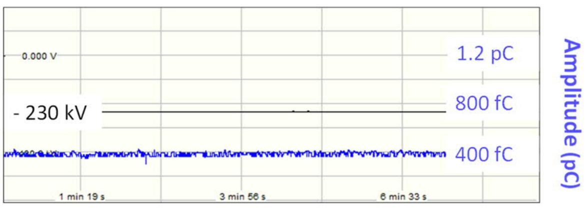

(a)

This project has received funding from the European Union's Horizon 2020 research and innovation programme under grant agreement No 691714.

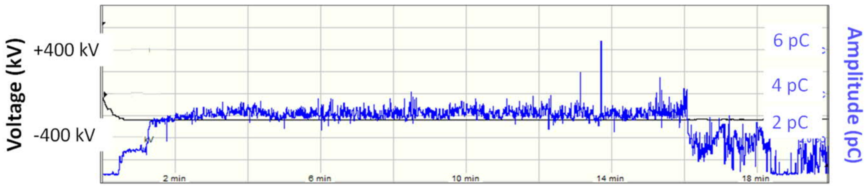

(b)

Figure 18: PD apparent charge before (a) and after (b) voltage interruption and reapplication. Measurement taken after 8 days under -230 kV in FN-CO2 10%.

Before voltage interruption, the recorded signal is only the ambient noise. However after the voltage interruption of 15 minutes, the PD apparent charge reaches a level of 3 pC at -230 kV(Figure 18(b)). When the voltage is constant, the PD apparent charges remains at this level during 15 minutes before decreasing to a lower level of about 1 pC and extinguish after. One can thus underline that the time of 15 minutes might be enough to relax charges deposited by metallic particle on solid surface in order to have PD activities again. This information is interesting to identify the time lap to perform PD measurement with this kind of defect. However, the time of 15 minutes is not constant, it depends on the applied polarity and gas nature. For example, in SF_6 in positive polarity, the interruption time must be more in the range of 1 h to relax deposited charges.

Finally, in real application where a voltage interruption is quite rare, the detection of the metallic particle on insulator surface is very challenging.

3.2.2 GAS COMPARISON

A comparison of the PD amplitude and PD repetition frequency with time of voltage application is very hard to obtain for this type of defect. The discharge activities were only detectable during the first minutes after the voltage application and then the discharges decreased quickly below ambient noise level or were extinguished. Some activities were registered again after some days but this behavior was difficult to record by our measuring systems due to fact that the PD measurement is conducted only some ten of minutes per day and not with a real time monitoring system. Moreover, the PD can reappear after a certain time of voltage interruption due to the surface charge relaxation phenomena. This behavior makes the comparison more difficult.

Nevertheless some general tendencies could be extrapolated from the test campaign, they are summarized in Table 2 below.

Table 2: Metallic partcile on solid insulator surface: gas comparsion regarding the PD amplirtude at the first voltage application, the maximum detected PD amplitude along all the voltage application time, the presence of discharges after the extinction and an estimation of the time needed for charge relaxation.

	DC+	DC-
	SF_6	
Initial PD amplitude (pC)	1.6	1.2
Max PD amplitude (pC)	3.5	1.6
Activity after extinction	Only after voltage stop/reapplication	Till 3 days, after 3 days no more activity

PROMOTioN – Progress on Meshed HVDC Offshore Transmission Networks

This project has received funding from the European Union's Horizon 2020 research and innovation programme under grant agreement No 691714.

Relaxation time	<1 h but rapid extinction	>>3 h (no PD reappearance if a stop of 3 h is applied)
	FN-CO2 10%	
Initial PD amplitude (pC)	1.5	1
Max PD amplitude (pC)	1.5	20-50
Activity after extinction	No more activity detected	Yes
Relaxation time	>>2 h (no PD reappearance if a stop of 2 h is applied)	<15 minutes
	FK-Air 6.6%	
Initial PD amplitude (pC)	6.5	4.2
Max PD amplitude (pC)	6.5	4.2
Activity after extinction	Only after voltage stop/reapplication	Only after voltage stop/reapplication
Relaxation time	<15/30 minutes very low amplitude	<30 minutes

One can note that the highest partial discharge amplitude has been measured for the FN-CO_2 10% mixture at negative polarity. Moreover either for the FN-CO_2 10% at positive polarity and SF_6 at negative polarity once the PD activity is extinguished after the first voltage application it is really difficult to relax the charges and have some PD activity again. For the FK-air 6,6% mixture the activity start at relatively high amplitude, in the order of 4-6 pC but then the discharge activity disappear quickly. It lasts only some minutes.

3.2.3 SUMMARY & REMARK

As observe in chapter 3.2.1 the measurement of the PD activity in presence of a metallic particle on solid insulator surface is very difficult. Indeed after the first moment of voltage application partial discharges can be detected but after some minutes the discharge activities decrease and extinguish. Afterward in some cases, due to charge relaxation, PD activities restart and PD pulses can be recorded again. However those discharges are in most of the cases with a really low amplitude and repetition frequency. It is thus very difficult for their detection. Only an effective real time monitoring system will ensure that those discharges will be detected.

As presented in chapter 3.1.3 the needles used for the long term test with a protrusion on HV conductor present sign of erosion or material pull out. It is thus interesting to evaluate the state of the defects also after the long term PD testing on solid insulator surface. One can note that the needles, reported in Figure 19 and in Figure 20 respectively for tests under negative and positive DC voltage, are mainly eroded. The needle tested under the 6.6%FK-air mixture presents sign of material pull out, see Figure 19 (c), similar to the one observed for the 10% FN-CO_2 mixture in Figure 13 (c). No particular correlation has been evidenced between the condition of the needles after tests and the maximum reached amplitude of the discharges.

This project has received funding from the European Union's Horizon 2020 research and innovation programme under grant agreement No 691714.

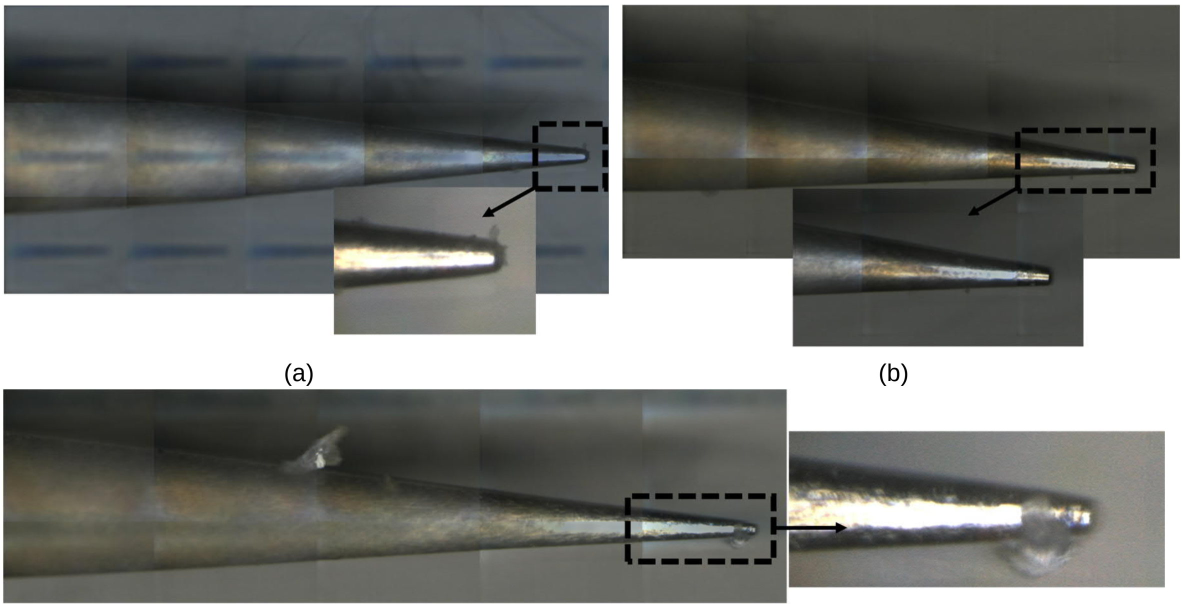

(a) (b)

(c)

Figure 19: Needles after PD long term test in solid insulator surface at negative polarity for different gases. (a) SF_6, (b) FN-CO_2 10% and (c) FK-Air 6.6%. Applied voltage: -230 kV.

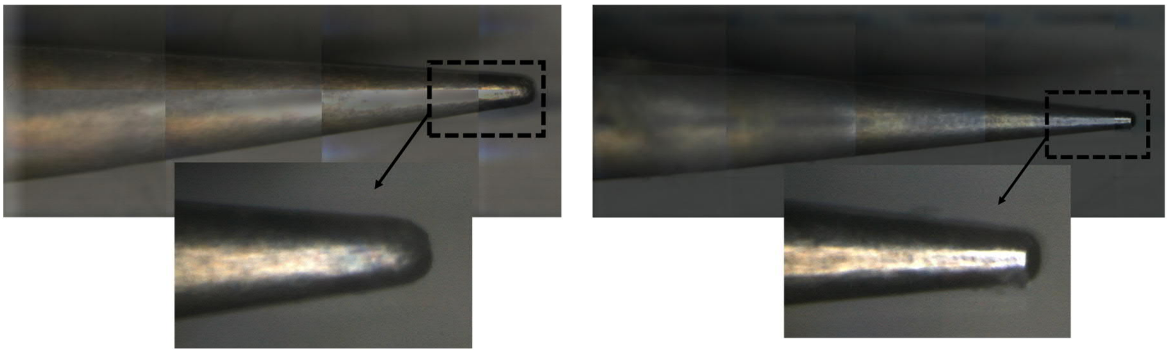

(a) (b)

Figure 20: Needles after PD long term test in solid insulator surface at positive polarity for different gases. (a) SF_6 and (b) FN-CO_2 10%. Applied voltage: +230 kV

This project has received funding from the European Union's Horizon 2020 research and innovation programme under grant agreement No 691714.

3.3 COMPARISON OF PD BEHAVIOR & MEASURING SYSTEMS

3.3.1 COMPARISON OF PD BEHAVIOR

First of all, one can observed that the pulse behavior is not the same between the two investigated defects: protrusion on high voltage conductor and metallic particle on insulator surface (Figure 21). The protrusion defect presents PD pulse with higher frequency components.

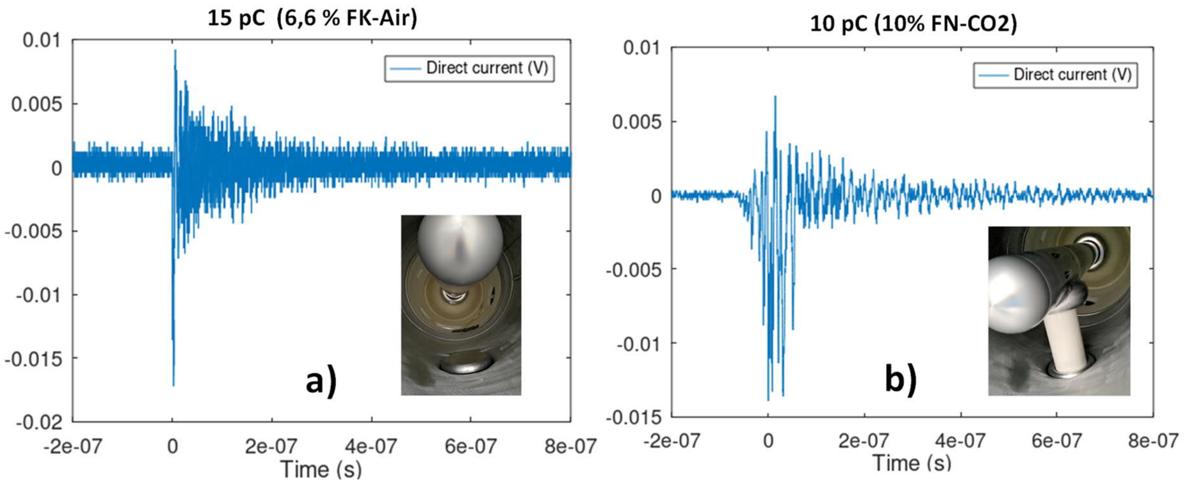

Figure 21: PD pulse signal recorded via 50 Ω resistor. (a) Protrusion defect and (b) Metallic particle on insulator surface

The difference in term of PD pulse might due to the formation of discharge. On one hand, the PD pulse is generated by the creation of an avalanche and thus space charges in front of the tip – protrusion defect. The phenomena are thus taking place in the gas and the discharge pulse presents high frequency components. On the other hand, when the defect is a metallic particle on insulator surface, the PD pulse is generated by the sum of avalanche activity in gas and also by charge emission from the dielectric surface. It leads to a lower frequency components of PD pulse.

The difference in term of frequency components can also be seen by other measuring systems. Figure 22 shows the signal recorded by different measuring systems for two kinds of defect. It should be noted that the maximum peaks of direct current measurement have a linear relationship with the PD apparent charge: 0.02 V for 15 pC - Figure 22(a) and 0.015 V for 10 pC - Figure 22(b). It can explained by the fact that the PD apparent charge calculation is based directly on the PD pulse current. However, for UHF measurement, as the sensor captures only the very high frequency components of PD pulse (above 300 MHz), a notable difference is denoted: the maximum amplitude of UHF signal is 0.01 V for protrusion defect and 0.002 V for metallic particle on insulator surface. The ratio between the maximum values of UHF signal is five time while the ratio between the PD apparent charges is only 1.5. It is in accordance with the observed pulse waveforms: higher frequency components presented for protrusion defect (Figure 21-a) leading to higher sensibility of the UHF method even though almost the same PD apparent charge is demonstrated for the two defects. On the other hand, with the magnetic sensor (TU Delft sensor) where the bandwidth is much lower than the UHF (in rage of 40 MHz), there is no sensitive difference between the signals recorded with protrusion defect and metallic particle on insulator surface: about

PROMOTioN – Progress on Meshed HVDC Offshore Transmission Networks

This project has received funding from the European Union's Horizon 2020 research and innovation programme under grant agreement No 691714.

0.2 V for one coil and 0.4 V for the different between the two pick-up coil. This observation can give some indicators/suggestion for bandwidth choice of PD sensor development.

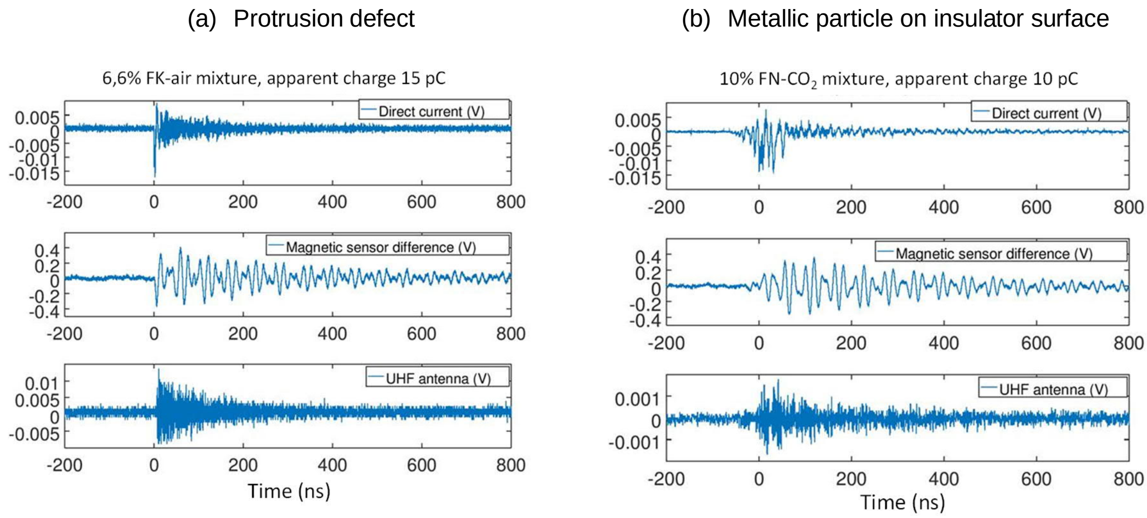

Figure 22: PD signals recorded by different measuring system. (a) Protrusion on high voltage conductor and (b) Metallic particle on insulator surface

3.3.2 COMPARISON OF MEASURING SYSTEMS

The conventional method with very low background noise (< 1 pC) rests an effective PD detection methods for all the conducted experiments with all the tested insulating gases. However, especially for the metallic particle on insulator surface, the PD amplitudes could be very small. It thus needs a perfect electromagnetic shielding protection, otherwise its detection capabilities are drastically impacted.

Pulse current measurements have shown a good detection capability and good sensitivity in our experiments. It is mainly due to the fact that the current pulse is directly collected in front of the defect with a special insulated electrode, something that is not possible in case of unknown defect position inside GIS.

The detection of the PD pulses by the UHF antenna remains a good solution to overcome a noisy environment but the experiments have shown that, depending on gas nature/composition and the defect type, the frequency content of the PD signal might be limited in the high frequency range. This affects the sensitivity of UHF method by the reduction of available resonance frequencies for defect detection.

The sensitivity to PD of the magnetic sensor seems to be, in our tests, as good as the UHF method. Indeed even if this sensor works at frequency range lower than the UHF method, thanks to its design with two pickup coils, it offers the possibility to subtract from the PD signal the external disturbances making it less sensitive to a high background noise environment. Moreover with this sensor, if a calibration procedure is performed on the complete measuring system [21], the computation of the apparent charge created by the defect might be possible. Further works are ongoing to have a better performance overview of different PD measuring systems, especially between UHF antenna and magnetic field sensor.

The main advantages and disadvantages of the studied PD measuring system in this test campaign are summarized in Table 3.

This project has received funding from the European Union's Horizon 2020 research and innovation programme under grant agreement No 691714.

Table 3: Comparison of different PD measuring systems.

	Pros	Cons
Conventional method	Effective method PD amplitude computable	Requires very high shielding level Requires coupling capacitor
Direct current	Effective method PD amplitude computable	Requires measuring electrode in front of defect
UHF	Immunity to environment noise	Less sensitive with low PD amplitude (lower than 2 pC) PD amplitude computation not possible
Magnetic sensor	PD amplitude computable	Less sensitive with low PD amplitude (lower than 2 pC) More sensitive to environment noise than UHF method but less than conventional method

This project has received funding from the European Union's Horizon 2020 research and innovation programme under grant agreement No 691714.

4 CONCLUSION

This document presents the experimental results about long term partial discharge behavior of defects under DC voltage. Two kind of defects: a protrusion on high voltage conductor and metallic particle on spacer surface and different gases SF_6, FN-CO_2 10% mixture, FK-Air 6.6% mixture with 5 bar SF_6 equivalent dielectric strength were investigated. Different measuring systems such as conventional method, UHF method and magnetic sensors were used. The long term PD behavior of different defects and a comparison of different gases were then reported.

For protrusion defect, the partial discharges are always detectable during all the investigated time. However, the PD amplitude and PD repetition frequency change with time. Depending on studied gas, the PD amplitude can remain constant with time or can increase before reaching a stabilized value after some days. Regarding the PD repetition frequency, it changes also with time and the tendency depends also on gas composition and voltage polarity. This study has underlined that the change of partial discharge behavior is not due to change of gas properties/compositions under DC voltage. It might be due to the modification of the defect as confirmed by the conducted microscope visual inspections after the tests.

For metallic particle on solid insulator surface, the detection of partial discharge activities is more difficult respect to the protrusion defect. Indeed with this type of defect the amplitude and repetition frequency, that are very low just after voltage application, decrease rapidly (~ minutes) with time till the extinction. Afterward in some cases, due to surface charge relaxation, PD activity restarts and PD pulses, with very low repetition frequency, can be recorded again. It is clear that the detection of this type of defect is very challenging and only an effective real time monitoring system, with high signal/noise ration can ensure the detection mission.

The effectiveness of the different applied measuring system, based on the performed test, has been briefly discussed and one can conclude that, even if some behavior difference has been underlined between SF_6 and the studied SF_6 alternatives, the replacement of SF_6 seems not to be an obstacle for an effective PD monitoring system.

This project has received funding from the European Union's Horizon 2020 research and innovation programme under grant agreement No 691714.

REFERENCES

[1] M. Kosse, K. Juhre, "Experience in testing of high voltage DC gas insulated systems and potential applications for rated voltages up to ±550 kV", Highvolt-Kolloquium 2019.
[2] T. Vu-Cong, G. Ortiz, F. Jacquier, P. Vinson and A. Girodet, "Design and validation test of 320 kV HVDC GIL/GIS", Matpost 2019.
[3] M. Gatzsche, U. Riechert, H. He, Y. Audichya, A. Rodrigo Mor, L. Castro Heredia, F. Muñoz. "Prototype Installation Test of HVDC GIS for Meshed Offshore Grids", CIGRE, 2020 SC B3 / PS1.
[4] A. Beroual and A. Haddad, "Recent advances in the quest for a new insulation gas with low impact on the environment to replace sulfur hexafluoride (SF6) gas in high voltage power network applications," Energies, vol. 10, pp. 1216, 2017.
[5] M. Rabie and C. M. Franck, "Comparison of gases for electrical insulation: fundamental concepts," IEEE Trans. Dielectr. Electr. Insul.,vol. 25, no. 2, pp. 649–656, Apr. 2018.
[6] E. Laruelle, Y. Kieffel and A. Ficheux, "g3- The alternative to SF6 for high voltage equipment", Eco-Design in Electrical engineering, 2017, pp.139-146.
[7] M. Hyrenbach, T. Hintzen, P. Muller, and J. Owens, "Alternative gas insulation in medium voltage switchgear," CIRED, 2015.
[8] L. Loizou, L. Chen, Q. Liu et al. "Technical Viability of Retro-filling C3F7CN/CO2Gas Mixtures in SF6-designed Gas InsulatedLines and Busbars at Transmission Voltages", IEEE transaction on power delivery, 2020.
[9] M. Claessens and F. Schober and M. Ahl, "Insulation performance of environmentally friendly fluoroketone based insulation gas mixtures", Proceedings of the 21st International Symposium on High Voltage Engineering, Volume 2, Oct. 2019.
[10] M. Aints, I. Jogi, M. Laan, P. Paris, and J. Raud, "Effective ionization coefficient of C5 perfluorinated ketone and its mixtures with air," J.Phys. D: Appl. Phys, 2019, vol. 51, pp. 135205.
[11] H. E. Nechmi, A. Beroual, A. Girodet, and P. Vinson, "Effective ionization coefficients and limiting field strength of fluoronitrile-CO2 mixtures," IEEE Trans. Dielectr. Electr. Insul., vol. 24, no. 2, pp. 886–892, Apr. 2017.
[12] G. Wang et al, "Green gas for grid as an eco-friendly alternative insulation gas to SF6: from the perspective of partial discharge under AC," Appl. Sci., vol. 9, pp. 651, 2019.
[13] B. Zhang, H. Uzelac, and Y. Cao, "Fluoronitrile/CO2 mixture as an ecofriendly alternative to SF6 in medium voltage switchgears," IEEE Trans. Dielectr. Electr. Insul., vol. 25, no. 4, Aug. 2018.
[14] A. Pirker and U. Schichler, "Partial discharges of defects in different insulating gases: N2, CO2, Dry air and SF6," IEEE Int. Conf. Prop. Appl. Dielectr. Mat. (ICPADM), 2018
[15] E. Ouss et al, "Measurement and analysis of partial discharge in HVDC gas insulated substations," Cigre Sci. Eng., vol. 11, pp. 62-69, 2018.
[16] PROMOTioN Project deliverable D15.7, "Report on PD characteristics of SF6 alternative gases: comparison with SF6", 2019.
[17] Cigré JWG D1/B3.57, "Dielectric testing of gas-insulated HVDC systems"
[18] WG 23.02 TB150, "Report on the second international survey on high voltage gas insulated substations (GIS) Service experience", CIGIRE, 2000
[19] High Voltage test techniques – Partial discharge measurements. IEC standard 60270: 2000, 2015-11.
[20] A. Rodrigo Mor, F. A. Muñoz Muñoz, L. C. Castro Heredia "A Novel Antenna for Partial Discharge Measurements in GIS Based on Magnetic Field Detection", Sensors 2019, 19, 858.
[21] A. Rodrigo Mor, L. C. Castro Heredia, F. A. Muñoz Muñoz "A magnetic loop antenna for partial discharge measurements on GIS", International Journal of Electrical Power & Energy Systems, Vol. 115, pp. 1-6, 2020.
[22] WG D1.25 TB654, "UHF partial discharge detection system for GIS: Application guide for sensitivity verification", CIGRE, 2016.
[23] C. Toigo, T. Vu-Cong, M. Dalstein, F. Jacquier, A. Girodet, A. Rodrigo Mor, L. Castro Heredia, F. Muñoz. "Measurement and behaviour of partial discharge for SF6 substitute gases in HVDC GIS/GIL", CIGRE, 2020 SC D1/ 837.

This project has received funding from the European Union's Horizon 2020 research and innovation programme under grant agreement No 691714.